

Unified theory of resonances and bound states in the continuum in Hermitian tight-binding modelsA. A. Gorbatsevich^{1,2,*} and N. M. Shubin²¹*P.N. Lebedev Physical Institute of the Russian Academy of Sciences, 119991, Moscow, Russia*²*National Research University of Electronic Technology, 124498, Zelenograd, Moscow, Russia*

(Received 20 July 2017; revised manuscript received 29 September 2017; published 28 November 2017)

We study the transport properties of an arbitrary two-terminal Hermitian system within a tight-binding approximation and derive an expression for the transparency in a form that enables one to determine the exact energies of the perfect (unity) transmittance, zero transmittance (Fano resonance), and bound state in the continuum (BIC). These energies correspond to the real roots of two energy-dependent functions that are obtained from two non-Hermitian Hamiltonians: the Feshbach effective Hamiltonian and the auxiliary Hamiltonian, which can be easily deduced from the effective one. BICs and scattering states are deeply interconnected. We show that the transformation of a scattering state into a BIC can be formally described as a “phase transition” with a divergent generalized response function. Design rules for quantum conductors and waveguides are presented. These rules describe the structures exhibiting coalescence of both resonances and antiresonances resulting in the formation of almost rectangular transparency and reflection windows. The results can find applications in the construction of molecular conductors, broad-band filters, quantum heat engines, and waveguides with controllable BIC formation.

DOI: [10.1103/PhysRevB.96.205441](https://doi.org/10.1103/PhysRevB.96.205441)**I. INTRODUCTION**

Resonance phenomena play a central role in the physics of open quantum systems and waveguides [1–3]. Therefore the ability to design structures with required resonance properties is of primary importance for the whole field of nanoelectronic and nanophotonic engineering. The past years demonstrated a steady progress in understanding the properties of open quantum systems (OQS) and subwavelength electronic and optical structures [1–4]. In simply connected structures, the main types of resonances are Fabry-Perot (FP) or Breit-Wigner (BW) resonances [5]. In multiply connected quantum systems, the interplay of different scattering paths can result in both constructive interference (resonances) and destructive interference (antiresonances).¹ If one of the paths includes a (quasi-) localized state, then an asymmetric Fano-Feshbach (FF) resonance is formed, which is composed of an antiresonance and a nearby resonance [3]. A traditional way to describe resonances is the scattering matrix (S -matrix) formalism [5,6]. The resonances correspond to the poles of the S matrix in the lower half of the complex energy plane [5]. S -matrix poles located on the real axis are related to bound states in the continuum (BIC), which therefore can be considered to be resonances with zero width. The existence of BICs was proposed on the eve of the quantum mechanics [7] but only recently BIC has been recognized as a wave phenomena [8] and a variety of approaches to realization of BIC have been studied [4] and experimentally verified [4,9]. The BIC amplitude can either monotonically decay away from its center

[7], as for an ordinary bound state, or occupy a restricted space region [10,11] being strictly zero outside it. In the latter case, BIC can be formed, for instance, between two FF scatterers, which form the FP resonator at the energy of FF resonance with zero transparency. In this case, the wave is trapped in the inner region and is completely destroyed by the destructive interference outside [10,12–14]. The total transparency of such structure is zero at the energy of FP BIC. Another type of spatially restricted BIC emerges at the point of collapse of resonance-antiresonance pair (Fano resonance) [15,16]. Transparency takes a finite nonzero value in this case.

The standard formalism of the quantum mechanics is based on Hermitian Hamiltonians. However, it is too complicated when applied for the description of OQS, because of the infinite environment, which should be also taken into account. The S -matrix approach is a way to overcome this difficulty. However, during the past decades a working OQS theory has been developed [1,6,17–19]. The theory operates with non-Hermitian Hamiltonians that could be obtained via Feshbach projection technique [6] from the parent Hermitian Hamiltonian describing both the quantum system and its environment. The amplitude of the S matrix can be explicitly expressed in terms of the Feshbach non-Hermitian effective Hamiltonian, the eigenvalues of which coincide exactly with the S -matrix poles and determine energies of resonant states [19,20]. Thus the physics of OQS becomes the physics of non-Hermitian Hamiltonians. Resonant states correspond to unstable states of OQS, they provide only outgoing waves without incoming ones, i.e., satisfy the Siegert boundary conditions. These states are very useful in, e.g., description of the nuclear reactions [19] or phase lapses in the transmission of quantum systems [21]. One of the advantages of this OQS theory is that it makes possible to elucidate subtle physical effects caused by the interference of the eigenfunctions of non-Hermitian Hamiltonians [22].

The resonant states that correspond to the eigenvalues of the non-Hermitian effective Hamiltonian should be distinguished from the scattering resonances, which are the main concern of

*aagor137@mail.ru

¹Throughout this paper we understand resonances and antiresonances as peaks and dips of the transmission coefficient at real energies. Specifically, we focus on the perfect resonances and antiresonances, i.e., scattering states with unity and zero transmission correspondingly (without taking into account imperfections and dissipation).

our paper. Scattering resonances are related to real energies, which determine the position of the transparency maxima on the real energy axis. However, the correspondence between the scattering resonances and the S -matrix poles is not trivial. For a narrow and isolated resonance, its location almost perfectly coincides with the real part of the pole of the scattering matrix (S matrix), while the imaginary part of the pole determines the resonance width. For wide and/or interacting (closely spaced) resonances, this is not true [23–25]. Interaction between the resonances can result in their coalescence (collapse of resonances [23,26]). For semiconductor heterostructures, it was described with two resonances [23,27] and for tunneling quantum dots three resonances were involved [28,29]. Collapse of eigenmodes was also observed in semiconductor cavities with the Rabi splitting [30], classical electrical circuits [31,32], quantum tunneling structures [33,34], etc. However, the coalescence of resonances can not be described by the behavior of the poles of the scattering matrix [23,29].

Implementation of novel physical concepts such as \mathcal{PT} -symmetry and \mathcal{PT} -symmetry breaking [35] (here \mathcal{P} and \mathcal{T} stand for the space inversion and time reversal symmetries, respectively) opened new directions in studying open electronic systems with non-Hermitian Hamiltonians [1,35] and electromagnetic waveguide structures with combined gain and loss [36,37]. It also shed a light on the mechanism of the coalescence of resonances. In Refs. [29,38–42], the relation between the resonances in quantum conductors and the \mathcal{PT} symmetry was studied. In fact, under the condition of the perfect resonance, incoming and outgoing particle flows are interrelated by the \mathcal{PT} symmetry. Therefore the \mathcal{PT} symmetry is inherent to the perfect resonance condition.

An important feature of \mathcal{PT} -symmetric systems is the \mathcal{PT} -symmetry breaking phenomenon, which takes place at some point of the parameter space, where two real eigenvalues coalesce and with further parameter variation turn into a pair of complex conjugated eigenvalues with nonzero imaginary parts [35]. Such point in the parameter space is known as the exceptional point (EP) [18,19,43–45]. The Hamiltonian at the EP takes the form of a Jordan matrix (which is obviously non-Hermitian). At the EP, the eigenvectors coalesce into a single nondegenerate state [18,19,43,46] as opposite to the case of the crossing (diaboloic) point, where they are degenerate and can be made orthogonal. It should be noted that, in general, the \mathcal{PT} symmetry of the non-Hermitian Hamiltonian is not a necessary and sufficient condition for energy spectrum to be real [47,48]. Because of the close mathematical similarity of the Schrödinger and wave equations, the \mathcal{PT} symmetry can be straightforwardly realized in optics, where \mathcal{PT} -symmetric terms correspond to the gain and loss regions. The \mathcal{PT} -symmetry breaking and EPs have been demonstrated in coupled waveguides [36], photonic lattices [49], \mathcal{PT} -symmetric plasmonic metamaterials [50,51], lasers [52], coherent perfect absorbers [53], and other optical systems.

In a fermionic system, time-odd terms in the Hamiltonian destroy unitarity. Nevertheless, one can realize non-Hermitian terms by inflow and outflow processes in a dissipationless open quantum system as it has been done in Ref. [40]. The same authors showed [41] that the scattering state of an arbitrary Hermitian lattice can be described as the eigenstate of an auxiliary non-Hermitian Hamiltonian with imaginary terms

that describe incoming and outgoing particle flows. Recently, within the framework of the tight-binding approximation, we have obtained the exact expression for the transparency of a dissipationless quantum chain (simply connected quantum conductor) [29,42], which directly relates the transparency maxima to the eigenvalues of an auxiliary non-Hermitian Hamiltonian that can be straightforwardly deduced from the Feshbach effective Hamiltonian. In some cases (e.g., in 1D spatially symmetric systems), an auxiliary Hamiltonian is \mathcal{PT} -symmetric and has real eigenvalues, which exactly determine the location of perfect resonances. At the EP of an auxiliary Hamiltonian, the resonances coalesce and a wide transparency window is formed. Transparency at the EP has a non-BW profile [23,42]. The poles of the scattering matrix (Green's function) can also coalesce and, as a result, a double pole is formed [24,54,55]. However, its location, in general, has no direct relation to the coalescence of resonances and, hence, to physical observables. Although, as shown in Refs. [56,57], the physical properties of the system do change at the EP of the scattering matrix of the system with balanced gain and loss, where two unimodular eigenvalues of the S matrix turn into two nonunimodular. In Ref. [54], the interaction between Fano resonances was analyzed in connection with the formation of the Green function double poles for interacting scattering channels, but just as in the case of the BW resonances, the location of a double pole has, in general, no relation to the location of the coalescence of resonances.

The energy (frequency) of BIC is the real eigenvalue of the effective Hamiltonian [4,58]. Due to unitarity of the S matrix (in a nondissipative system), some relations should exist between the zeros of the denominator (eigenvalues of the effective Hamiltonian) and the zeros of the numerator (antiresonances) in the expression for the S matrix, which has been recently studied on phenomenological grounds in Ref. [59]. On the other hand, the zeros of the effective Hamiltonian in the complex plane determine resonances. Hence the resonances and BIC energies (frequencies) are interrelated as well.

In the present paper, we generalize the result of Ref. [29] for an arbitrary two-terminal Hermitian system. We show that the scattering properties (transmission coefficient) of such systems can be described by two energy-dependent functions, which are derived from the effective Hamiltonian and another non-Hermitian Hamiltonian—the auxiliary Hamiltonian. Opposite to the effective Hamiltonian, this approach allows one to find *exact* perfect and zero transmission energies (frequencies) even for closely located and overlapping resonances. Moreover, the microscopic theory presented here provides a unified description of transparency maxima (resonances), transparency zeros (antiresonances), and BIC energies (frequencies) as well.

The structure of the paper is as follows. The model under consideration is described in Sec. II. In Sec. III, within a tight-binding approximation, we derive a formula for the transparency of an arbitrary two-terminal multiply connected molecular (or QD) conductor or waveguide. In Sec. IV, we show that the transition to a BIC state in the parameter space is characterized by the singularity of the generalized response function just as in the case of the second-order phase transition. However, the formation of the BIC state is discontinuous. In Sec. V, we present the models that demonstrate the coalescence

of Fano resonances either at the EP or crossing points, which is accompanied by the formation of wide reflection windows. A summary is made in Sec. VI.

II. GENERAL RELATIONS: MODEL AND TRANSMISSION COEFFICIENT

We consider an arbitrary N -site Hermitian structure connected to two semi-infinite leads. Every isolated site is assumed to have a single localized state with a real energy ε_i . Within the tight-binding approximation this system can be described by the Hamiltonian

$$\hat{H} = \hat{H}_0 + \hat{H}_L + \hat{H}_R + \hat{H}_{\text{int}}^L + \hat{H}_{\text{int}}^R. \quad (1)$$

The first term in (1) describes an isolated Hermitian N -site structure:

$$\hat{H}_0 = \sum_{i=1}^N \varepsilon_i a_i^\dagger a_i + \sum_{i,j=1,i<j}^N (\tau_{ij} a_j^\dagger a_i + \text{H.c.}), \quad (2)$$

where $a_i^\dagger(a_i)$ is the creation (annihilation) operator of the electron on the i th site and τ_{ij} is the tunneling matrix element between the i th and the j th sites. We consider here a single-electron problem without taking into account many-body effects such as electron-electron interaction, electron-phonon scattering, etc. Neglecting electron-electron Coulomb and exchange interactions limits us to the case of small on-site amplitudes and fast tunneling rates in order to prevent charge accumulation.

The Hamiltonian (1) is also applicable to the description of optical waveguide systems within an evanescent wave coupling approximation. In the case of an optical system, we consider light propagation along waveguides (instead of time evolution in a quantum system); the on-site energies and tunneling matrix elements are replaced by the corresponding propagation constants and evanescent field overlapping integrals [60,61]. In contrast to electron systems, here there is no restriction on the field amplitudes.

Leads with the energy spectrum $\varepsilon_{L(R)} = \varepsilon_{L(R)}(p)$ are described by the Hamiltonians \hat{H}_L and \hat{H}_R :

$$\hat{H}_{L(R)} = \sum_p \varepsilon_{L(R)}(p) a_{L(R),p}^\dagger a_{L(R),p}. \quad (3)$$

Operator $a_{L(R),p}$ in (3) corresponds to the state in the left (right) lead with momentum p . Term $\hat{H}_{\text{int}}^{L(R)}$ in Eq. (1) describes the interaction between the state with momentum p in the left (right) lead and the i th site of the structure:

$$\hat{H}_{\text{int}}^{L(R)} = \sum_{p,i} (\gamma_{p,i}^{L(R)} a_i^\dagger a_{L(R),p} + \text{H.c.}). \quad (4)$$

Here, $\gamma_{p,i}^{L(R)}$ is the matrix element, which, in general, is energy- and momentum-dependent.

The transport properties of the quantum system are governed by its transmission coefficient, which can be written as [62,63]

$$T = 4 \text{Tr}(\hat{\Gamma}^R \hat{G}^r \hat{\Gamma}^L \hat{G}^a). \quad (5)$$

Here, \hat{G}^r and $\hat{G}^a = (\hat{G}^r)^\dagger$ are correspondingly the retarded and advanced Green functions of the system. Taking the interaction

with the leads into account, we have

$$\hat{G}^r = (\omega \hat{I} - \hat{H}_{\text{eff}})^{-1}, \quad (6)$$

where \hat{I} is the $N \times N$ identical matrix and \hat{H}_{eff} is the effective Hamiltonian [6] of the structure:

$$\hat{H}_{\text{eff}} = \hat{H}_0 + \hat{\Sigma}^L + \hat{\Sigma}^R. \quad (7)$$

Here, $\hat{\Sigma}_{L(R)}$ is the self-energy of the left (right) lead. The Hermitian matrix $\hat{\Gamma}^{L(R)}$ from Eq. (5) describes the anti-Hermitian part of the corresponding lead self-energy:

$$\hat{\Sigma}^{L(R)} = \hat{\delta}^{L(R)} - i\hat{\Gamma}^{L(R)}. \quad (8)$$

In the system, we consider elements of $\hat{\delta}^{L(R)}$ and $\hat{\Gamma}^{L(R)}$ matrices, which can be easily deduced by standard methods [64] under the assumption that $\gamma_{p,i}^{L(R)} = \gamma_i^{L(R)}(\omega)$ depends only on energy, rather than on momentum.

Thus the transmission coefficient of the structure becomes

$$T = \frac{4 \sum_{i,j,m,k=1}^N (-1)^{i+j+m+k} M_{ij}^* M_{mk} \Gamma_{jk}^R \Gamma_{mi}^L}{|\det(\omega \hat{I} - \hat{H}_{\text{eff}})|^2}. \quad (9)$$

Minors M_{ij} in Eq. (9) are the minors of the $(\omega \hat{I} - \hat{H}_{\text{eff}})$ matrix.

III. GENERALIZED FORMULA FOR TRANSMISSION COEFFICIENT

In Ref. [29], it was shown that in the model of a simply connected quantum conductor (quantum chain) the denominator and the numerator in Eq. (9) are connected by a simple relation, which makes it possible to determine the exact positions of the perfect transparency energies on the energy axis. The derivation of this result was based on the properties of tridiagonal matrices. Here we present a much more general way of deriving that result and show that the analogous decomposition of the squared module of the characteristic determinant of the effective Hamiltonian can be performed for an arbitrary multiply connected quantum conductor described by model (1). This property provides separate control over the transparency peaks and dips.

Matrix $\hat{\Gamma}^{L(R)}$ can be written in the following form [65]:

$$\hat{\Gamma}^{L(R)} = \mathbf{u}_{L(R)} \mathbf{u}_{L(R)}^\dagger, \quad (10)$$

with vector $(\mathbf{u}_{L(R)})_i = \sqrt{\pi \rho_{L(R)}} \gamma_i^{L(R)}$, where $\rho_{L(R)}$ is the density of states in the leads. Using Eq. (10), we can simplify Eq. (5) in a way different from that in Eq. (9). Let us introduce a matrix

$$\hat{A} = \omega \hat{I} - \hat{H}_0 - \hat{\delta}^L - \hat{\delta}^R. \quad (11)$$

Matrix \hat{A} is Hermitian and this property is crucial for further calculations. Using \hat{A} from Eq. (11) we can simplify the transmission coefficient to the following:

$$\begin{aligned} T &= 4 \text{Tr}\{\mathbf{u}_R \mathbf{u}_R^\dagger (\hat{A} + i\mathbf{u}_L \mathbf{u}_L^\dagger + i\mathbf{u}_R \mathbf{u}_R^\dagger)^{-1} \\ &\quad \times \mathbf{u}_L \mathbf{u}_L^\dagger [(\hat{A} + i\mathbf{u}_L \mathbf{u}_L^\dagger + i\mathbf{u}_R \mathbf{u}_R^\dagger)^{-1}]^\dagger\} \\ &= 4 |\mathbf{u}_R^\dagger (\hat{A} + i\mathbf{u}_L \mathbf{u}_L^\dagger + i\mathbf{u}_R \mathbf{u}_R^\dagger)^{-1} \mathbf{u}_L|^2. \end{aligned} \quad (12)$$

Then applying the Sherman-Morrison formula [66] and matrix determinant lemma [67], we can simplify (12) and get

$$T = \frac{4 |\det \hat{A}|^2 |\mathbf{u}_R^\dagger \hat{A}^{-1} \mathbf{u}_L|^2}{|\det(\hat{A} + i\mathbf{u}_L \mathbf{u}_L^\dagger + i\mathbf{u}_R \mathbf{u}_R^\dagger)|^2}. \quad (13)$$

According to the definitions (10) and (11), the denominator of Eq. (13) is nothing more than the characteristic determinant of the effective Hamiltonian, which is also present in the denominator of Eq. (9) for the transmission coefficient. Hence the numerators of Eqs. (13) and (9) should coincide as well. From Eq. (13), it follows that the numerator of the transmission coefficient is a square module of a certain energy-dependent quantity P , which is defined up to an arbitrary phase factor:

$$P = 2\mathbf{u}_R^\dagger (\text{adj } \hat{A}) \mathbf{u}_L. \quad (14)$$

Here, $\text{adj } \hat{A}$ is the adjugate matrix of \hat{A} from Eq. (11).

Now we isolate the term $4|\det \hat{A}|^2 |\mathbf{u}_R^\dagger \hat{A}^{-1} \mathbf{u}_L|^2 = |P|^2$ in the denominator of Eq. (13) and then we just simplify the rest of the denominator. Applying the matrix determinant lemma once again one can figure out that

$$\begin{aligned} |\det(\omega \hat{I} - \hat{H}_{\text{eff}})|^2 &= |\det(\hat{A} + i\mathbf{u}_L \mathbf{u}_L^\dagger + i\mathbf{u}_R \mathbf{u}_R^\dagger)|^2 \\ &= |P|^2 + |Q|^2, \end{aligned} \quad (15)$$

where Q is another function of ω defined up to an arbitrary phase factor:

$$Q = \det(\hat{A} - i\hat{\Gamma}^L + i\hat{\Gamma}^R). \quad (16)$$

Quantity Q can be understood as a characteristic determinant of some auxiliary Hamiltonian \hat{H}_{aux} :

$$\hat{H}_{\text{aux}} = \hat{H}_0 + \hat{\delta}^L + \hat{\delta}^R + i\hat{\Gamma}^L - i\hat{\Gamma}^R. \quad (17)$$

This auxiliary Hamiltonian differs from the effective one (7) only in the sign of $\hat{\Gamma}^L$ or $\hat{\Gamma}^R$. The choice of the sign is arbitrary, but for the sake of convenience, it can be preassigned with the direction of the current flow taken into account. According to this, the auxiliary Hamiltonian corresponds to the scattering boundary conditions, i.e., outgoing waves produced by an incoming one, rather than to the Siegert boundary conditions as the Feshbach effective Hamiltonian does. Non-Hermitian Hamiltonians with such boundary conditions (scattering) naturally appear in the description of the scattering states with perfect transmission [29,40–42].

Substituting Eq. (15) into Eq. (13), one can get the expression for the transmission coefficient of an arbitrary two-terminal Hermitian structure in the following form:

$$T = \frac{|P|^2}{|P|^2 + |Q|^2}. \quad (18)$$

This formula for the linear chain structures (simply connected) was derived in Ref. [29] and here it is shown to hold true in a much more general case (multiply connected). Equations (17) and (18) represent the main result of this section. In fact, we have proven the theorem that the transmission coefficient can be expressed in terms of two characteristic determinants of two non-Hermitian Hamiltonians. One is the effective Hamiltonian (7), the other is the auxiliary Hamiltonian (17), which can be deduced from the effective one. Hence formula (18) can be also written as

$$T = \frac{|\omega \hat{I} - \hat{H}_{\text{eff}}|^2 - |\omega \hat{I} - \hat{H}_{\text{aux}}|^2}{|\omega \hat{I} - \hat{H}_{\text{eff}}|^2}. \quad (19)$$

Thus, according to the close relation between the effective and auxiliary Hamiltonians [see Eqs. (7) and (17)], one can see

from Eq. (19) that the transmission probability of the system can be fully described by the effective Hamiltonian only. It is worth mentioning that a standard normalized Fano resonance profile [68]

$$T(\omega) = \frac{1}{1+q^2} \frac{(\omega+q)^2}{1+\omega^2} \quad (20)$$

can be easily rewritten in the form (18) with $|P|^2 = (\omega+q)^2$ and $|Q|^2 = (\omega q - 1)^2$.

The eigenvalue problem for the Hamiltonian \hat{H}_{aux} is nonlinear due to self-energies and, consequently, it should be solved self-consistently. This fact can have a serious impact on its properties [69]. Strictly speaking, this means that, in general, Q and P are not polynomials. However, if one neglects the dependence of the self-energy terms on the energy, then Q and P can be considered as polynomials [29].

According to Eq. (18), unity values of the transmission coefficient exactly coincide with the real roots of Q , i.e., with the real eigenvalues of the auxiliary Hamiltonian. Moreover, Eq. (18) enables one to determine exactly the positions of zero transmittance. Indeed, zero values of the transmission coefficient coincide with the real roots of P . However, as it will be shown further, not all of the real roots of Q correspond to the unity transmittance and not all real roots of P correspond to zero transmittance as the roots of P and Q can coincide (which is just the case for BIC).

It should be noted here that the approach of describing the exact positions of resonances and antiresonances, presented in this paper, has no restrictions both on the complex tunneling matrix elements τ_{ij} inside the structure and on the complex couplings $\gamma_i^{L(R)}$ with the leads. Consequently, all phase shifts of hopping integrals $\Delta\phi = \frac{e}{\hbar} \int_{\text{tunnel.path}} \mathbf{A} \cdot d\mathbf{l}$ induced by an external electromagnetic field with a vector potential \mathbf{A} can be taken into account properly allowing for the description of the Aharonov-Bohm effect [70]. Thus, for instance, numerical analysis of several quantum dot-based interferometers [15,16,71] can be extended to an explicit analytical description.

The expressions for the transmission coefficient derived above can be simplified dramatically if we consider that each lead interacts only with one site of the structure. Indeed, suppose that the left lead is attached to the site number 1 and the right lead to the site number N . In this case, each of the matrices $\hat{\Gamma}^{L(R)}$ and $\hat{\delta}^{L(R)}$ possess only one nonzero element each. For the leads modeled by semi-infinite linear chains, these quantities can be calculated explicitly [26,64,72]. Moreover, in this case, the point contact approximation can be applied even if the interaction with the lead is nonlocal, the only requirement is that only a finite number of sites in the lead interact with the system.

In the point interaction approximation, the functions P and Q are reduced to

$$\begin{aligned} P &= 2\sqrt{\Gamma_L \Gamma_R} M_{N1}, \\ Q &= \det(\omega \hat{I} - \hat{H}_{\text{aux}}), \end{aligned} \quad (21)$$

where M_{N1} is the minor of the $(\omega \hat{I} - \hat{H}_{\text{eff}})$ matrix, \hat{H}_{eff} is the effective Hamiltonian:

$$\begin{aligned} (\hat{H}_{\text{eff}})_{mn} &= (\hat{H}_0)_{mn} + (\delta_L - i\Gamma_L) \delta_{m1} \delta_{n1} \\ &\quad + (\delta_R - i\Gamma_R) \delta_{mN} \delta_{nN}, \end{aligned} \quad (22)$$

and \hat{H}_{aux} is the auxiliary Hamiltonian:

$$\begin{aligned} (\hat{H}_{\text{aux}})_{mn} = & (\hat{H}_0)_{mn} + (\delta_L + i\Gamma_L)\delta_{m1}\delta_{n1} \\ & + (\delta_R - i\Gamma_R)\delta_{mN}\delta_{nN}. \end{aligned} \quad (23)$$

Here, $\delta_{L(R)}$ and $\Gamma_{L(R)}$ are nonzero elements of the corresponding contact self-energy matrices. The feature of Eq. (21) is that the minor M_{N1} turns out to be independent of $\delta_{L(R)}$ and $\Gamma_{L(R)}$. Thus we can treat M_{N1} here as the minor of the $(\omega\hat{I} - \hat{H}_0)$ matrix. This approximation of point interaction with the leads will be used in Secs. IV and V.

IV. BOUND STATES IN THE CONTINUUM

A. General properties of P and Q functions at BIC

The bound state in the continuum (BIC) is a localized state with the energy lying within the energy interval of continuum states [4]. BICs are nondecaying states, hence, they do not interact with continuum and, therefore, have zero width. Such states correspond to real eigenvalues of the effective Hamiltonian lying within the energy band of the leads. In Refs. [15,16,73,74], BICs in some particular QD systems were identified by the presence of a δ -function peak in the density of states (DOS). This result can be generalized for an arbitrary two-terminal system (see Appendix A for details). Here we discuss the connection between BICs and the properties of P and Q functions.

Suppose effective Hamiltonian \hat{H}_{eff} has a real eigenvalue $\omega = \omega_0$:

$$\det(\omega\hat{I} - \hat{H}_{\text{eff}}) \propto (\omega - \omega_0). \quad (24)$$

According to Eq. (15) it follows from (24) that

$$|P(\omega)|^2 + |Q(\omega)|^2 = |\det(\omega\hat{I} - \hat{H}_{\text{eff}})|^2 \propto (\omega - \omega_0)^2. \quad (25)$$

At $\omega = \omega_0$, the sum of two non-negative quantities takes a zero value, hence, they are both zero. Therefore

$$P, Q \propto (\omega - \omega_0), \quad (26)$$

and we can conclude that there is BIC in the system if and only if the P and Q share the same real root.

These simple considerations, based on the introduction of the auxiliary Hamiltonian, show that the presence of BIC at the energy ω_0 implies the presence of the root of P at the same energy. Thus, according to Eqs. (9) and (18), the problem of divergence of transmission at the BIC energy, discussed, for example, in Ref. [59], is resolved easily. On the other hand, the reverse is *not* true and the presence of a real root of P does not imply that there is BIC. Shortly, one can formulate different possibilities as follows: (1) there is a unity-valued resonance at the energy ω_0 , if $P(\omega_0) \neq 0$ and $Q(\omega_0) = 0$. (2) There is a zero-valued antiresonance at the energy ω_0 , if $P(\omega_0) = 0$ and $Q(\omega_0) \neq 0$. (3) There is a BIC at the energy ω_0 , if $P(\omega_0) = 0$ and $Q(\omega_0) = 0$.

In a more general case, suppose that the energy ω_0 is a root of multiplicity m_Q of Q and also it is a root of multiplicity m_P of P . Then there are $\min(m_Q, m_P)$ degenerate BICs at the energy ω_0 and $m_Q - m_P$ coalesced resonances, if $m_Q > m_P$, or $m_P - m_Q$ coalesced antiresonances, if $m_Q < m_P$. If $m_Q = m_P$, then there are no extreme points of transmission at all. In other words, using P and Q functions

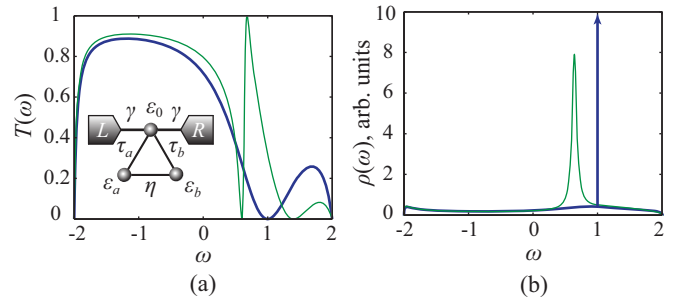


FIG. 1. BIC at zero transmission energy. (a) Transmission coefficient of a three-site system within tight-binding approximation with $\eta = 0.4$ (thin green line) and $\eta = 0$ (thick blue line). (Inset) Schematic view of three-site structure considered. (b) DOS for this structure [parameters are the same as in part (a)]. At $\eta = 0$, BIC appears and manifests itself as δ -function peak in DOS. All values are in units of J .

we just easily demonstrated that BIC is indeed a zero width resonance. According to expression (18), one can see that condition $Q(\omega_0) = 0$ indicates that BIC is a resonance and $P(\omega_0) = 0$ implies that it has zero width. Therefore BICs can appear because of resonance-antiresonance coalescence. This phenomenon was studied in the literature for particular quantum systems [10,73,75–77]. In the following section, we illustrate this conclusion.

B. Resonances and BICs in toy three-site model

In this section, we consider resonances, antiresonances, and BICs in a simple three-site structure [see the inset in Fig. 1(a)]. The Hamiltonian of the structure has the form (1) with the particular parameters defined below. We assume the leads to be identical semi-infinite linear chains with equal on-site energies set as the energy origin and the nearest-neighbor hopping integrals J set as the energy unit. These leads we treat to be attached locally to the site 0 of the structure via equal tunneling matrix elements $\gamma_0^L = \gamma_0^R = \gamma \in \mathbb{R}$. Tunneling matrix elements τ_a , τ_b , and η are real and of the same sign, e.g., positive and the on-site energies of the structure are taken to be $\epsilon_0 = 0$ and $\epsilon_a = \epsilon_b = \epsilon$. Thus the explicit expressions for the functions P and Q are

$$\begin{aligned} P &= \gamma^2 \sqrt{4 - \omega^2} (\omega - \epsilon - \eta)(\omega - \epsilon + \eta), \\ Q &= (\omega - \epsilon + \eta)^3 (1 - \gamma^2) + (\omega - \epsilon + \eta)^2 (\epsilon - 3\eta)(1 - \gamma^2) \\ &\quad + (\omega - \epsilon + \eta) [2\eta(\eta - \epsilon)(1 - \gamma^2) - \tau_a^2 - \tau_b^2] \\ &\quad + \eta(\tau_a - \tau_b)^2. \end{aligned} \quad (27)$$

P has two real roots $\omega = \epsilon \pm \eta$, which coincide with the energies of the eigenstates of QD molecule formed by sites a and b . Another two roots, $\omega^2 = 4$, correspond to the leads band edges where the particle velocity and, hence, the transparency turn into zero. BIC occurs if and only if Q shares roots with P . According to Eq. (27), only the root $\omega = \epsilon - \eta$ can be common for P and Q and this takes place as soon as $\tau_a = \tau_b$ or $\eta = 0$. If τ_a and τ_b were of opposite signs, there would be BIC at $\tau_a = -\tau_b$ with the energy $\omega = \epsilon + \eta$. This BIC

has properties similar to that at $\tau_a = \tau_b$ and with the energy $\omega = \varepsilon - \eta$, thus, we will not consider it in this paper. The multiplicities m_P and m_Q of the roots of P and Q can vary and in the following sections we consider different cases of BIC formation, depending on these multiplicities.

This structure possess conventional bound states with exponential decaying asymptotics: $a_n^{L(R)} \propto e^{-\kappa|n|}$. However, the energies of these bound states are beyond the continuum; they are referred to as bound states outside the continuum (BOC). On the other hand, there may exist the BICs with all the site amplitudes equal zero except for a and b . The relation between these nonzero amplitudes is established as

$$\tau_a a + \tau_b b = 0, \quad \text{for } \eta = 0, \quad (28)$$

$$a + b = 0, \quad \text{for } \tau_a = \tau_b. \quad (29)$$

To find the particular values for a and b in each case one can normalize the corresponding state as a conventional bound state. As we see from (28) and (29), the BIC amplitude distribution is antisymmetric for $\tau_a = \tau_b$. According to the

standard BIC classification [4,77], one can easily check that both Eqs. (28) and (29) describe the Friedrich-Wintgen BIC [8], i.e., the BIC formed by the destructive interference between two states coupled to the same continuum. Any other system possessing BICs can be studied in the same manner,² e.g., Fano mirror BICs described in Refs. [10,12–14].

The site amplitudes of the scattering state in this structure can be easily calculated by solving the corresponding tight-binding Schrödinger equation with the boundary conditions given by $a_n^L = e^{ikn} + r e^{-ikn}$ for the left lead and $a_n^R = t e^{ikn}$ for the right lead, where r and t are the reflection and transmission amplitudes respectively. Taking into account the dispersion relation for the leads ($\omega = -2 \cos k$) one can derive the site amplitudes of the scattering state:

$$\begin{aligned} a_0 &= C(\omega - \varepsilon - \eta)(\omega - \varepsilon + \eta), \\ a &= C[\tau_a(\omega - \varepsilon + \eta) - \eta(\tau_a - \tau_b)], \\ b &= C[\tau_b(\omega - \varepsilon + \eta) - \eta(\tau_b - \tau_a)], \end{aligned} \quad (30)$$

where

$$C = \frac{i\gamma\sqrt{4 - \omega^2}}{(\omega - \varepsilon + \eta)\{(\omega - \varepsilon - \eta)[\omega - \gamma^2(\omega - i\sqrt{4 - \omega^2})] - \tau_a^2 - \tau_b^2\} + \eta(\tau_a - \tau_b)^2}.$$

From (30), it follows that either at the BIC or at antiresonance energy (both corresponding to $P = 0$) the site amplitude a_0 always equals zero.

1. $m_Q < m_P$

For our particular structure, described above, the condition $m_Q < m_P$ can be fulfilled only for $m_Q = 1$ and $m_P = 2$, which, in turn, requires $\eta = 0$. In this case, BIC forms at the energy of zero transmittance $\omega = \varepsilon$. Figure 1 depicts the plots of the transmission coefficient and DOS for $\eta = 0$ and for $\eta \neq 0$. For illustration, we take $\gamma = 1$, $\tau_a = 1$, $\tau_b = 0.5$, and $\varepsilon = 1$. According to Appendix A, formation of BIC manifests itself as a δ -function peak of DOS.

Now consider the site amplitudes of the scattering state in the vicinity of this BIC. According to Eq. (30) at the energy $\omega = \varepsilon$ there are no special features of the site amplitude distribution for any values of η and even for $\eta = 0$, corresponding to BIC formation. Nevertheless, from the direct analysis of Eq. (30) one can figure out that at the energy $\omega = \varepsilon'$, where

$$\varepsilon' = \varepsilon - 2\eta \frac{\tau_a \tau_b}{\tau_a^2 + \tau_b^2}, \quad (31)$$

the site amplitudes of the scattering state become [written as a vector (a_0, a, b)]

$$\begin{aligned} (a_0, a, b) &= \frac{i\gamma(\tau_a^2 + \tau_b^2)\sqrt{4 - \varepsilon'^2}}{(\tau_a^2 - \tau_b^2)[\varepsilon'(1 - \gamma^2) + i\gamma^2\sqrt{4 - \varepsilon'^2}]} \\ &\times \left(\frac{\tau_a^2 - \tau_b^2}{\tau_a^2 + \tau_b^2}, \frac{\tau_b}{\eta}, -\frac{\tau_a}{\eta} \right). \end{aligned} \quad (32)$$

As one can see from Eq. (32), the distribution of the scattering state amplitudes a and b satisfies the relation (28), consequently, it corresponds to the BIC state except for a_0 is nonzero. In the limit $\eta \rightarrow 0$, amplitudes on the sites a and b formally diverge, whereas the amplitude on the site a_0 remains constant. Thus the interrelation between site amplitudes (symmetry) tends to that of the BIC state, i.e., defined by Eq. (28). On the other hand, at the exact BIC condition ($\eta = 0$ and $\omega = \varepsilon$) the amplitudes are

$$(a_0, a, b) = -\frac{i\gamma\sqrt{4 - \varepsilon^2}}{\tau_a^2 + \tau_b^2}(0, \tau_a, \tau_b). \quad (33)$$

From Eq. (33), one can see that the distribution of the scattering state site amplitudes (a and b) at the exact BIC condition abruptly changes and becomes orthogonal to BIC.

2. $m_Q = m_P$

When $m_Q = m_P$, BIC forms at the energy, corresponding to a nonextreme point of the transmission. For the structure we consider, the only possible case is $m_Q = m_P = 1$. According to Eq. (27), this requires P and Q to be linear in $(\omega - \varepsilon + \eta)$; this can be satisfied if $\tau_a = \tau_b$ and $\eta \neq 0$. For instance, let us take $\eta = 1 \neq 0$, $\gamma = 1$, $\tau_a = \tau_b = 1$, and $\varepsilon = 1$. In this particular case, BIC forms at the energy $\omega = \varepsilon - \eta = 0$. Figure 2 shows the transmission coefficient and DOS for the three-site structure with $\tau_a = \tau_b$ and with $\tau_a \neq \tau_b$.

At the exact energy of this BIC ($\omega = \varepsilon - \eta$), as can be deduced from Eq. (30), the scattering state amplitudes (a_0, a, b)

²See Ref. [78] for the application of the theory to several models of BIC formed in a Fabry-Perot resonator.

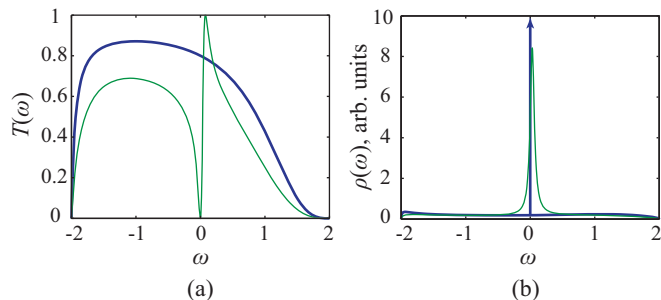


FIG. 2. BIC at “annihilation point” of Fano resonance-antiresonance pair with nonzero transmission. (a) Transmission coefficient of three-site system within tight-binding approximation with $\tau_a = 1.5$ (thin green line) and $\tau_a = 1$ (thick blue line). (b) DOS for this structure [parameters are the same as in part (a)]. At $\tau_a = 1$, BIC appears and manifests itself as δ -function peak in DOS. All values are in units of J .

are excited in an antisymmetric way:

$$a_0 = 0, \quad a = -b = \frac{i\gamma\sqrt{4 - (\varepsilon - \eta)^2}}{\tau_b - \tau_a}. \quad (34)$$

This distribution fully coincides in symmetry with the corresponding BIC (29). In the limit $\tau_a \rightarrow \tau_b$, the amplitudes a and b formally diverge. However, in the exact BIC regime ($\tau_a = \tau_b$) and at the energy $\omega = \varepsilon - \eta$, as can be seen from Eq. (30), the scattering state amplitudes (a_0, a, b) are

$$(a_0, a, b) = -\frac{i\gamma\sqrt{4 - (\varepsilon - \eta)^2}}{2\eta[\varepsilon - \eta - \gamma^2(\varepsilon - \eta - i\sqrt{4 - (\varepsilon - \eta)^2})] - 2\tau_a^2} \times (0, \tau_a, \tau_a). \quad (35)$$

According to Eq. (35), a and b site amplitudes are distributed symmetrically and are orthogonal to BIC.

3. $m_Q > m_P$

For $m_Q > m_P$, BIC forms at the energy of the perfect transmission. For the particular structure, we consider this can take place only for $m_Q = 2$ and $m_P = 1$. In this case, P should be linear and Q should be quadratic on $(\omega - \varepsilon + \eta)$. Thus, from Eq. (27), we deduce that $\eta \neq 0$ and $\tau_a = \tau_b = \sqrt{\eta(\eta - \varepsilon)(1 - \gamma^2)}$. In order to have a nondisjoint structure (τ_a and τ_b cannot vanish simultaneously), we also should restrict ourselves with $\eta > \varepsilon$ and $\gamma < 1$ (or $\eta < \varepsilon$ and $\gamma > 1$). As an example, let us take $\eta = 1 \neq 0$, $\varepsilon = 0.5 < \eta$, and $\gamma = 0.5 < 1$, hence, we have $\tau_a = \tau_b = \frac{\sqrt{3}}{2\sqrt{2}}$. At these conditions, BIC forms at the energy $\omega = \varepsilon - \eta = -0.5$. Figure 3 illustrates this by plots of the transmission coefficient and DOS at $\tau_a = \tau_b$ and at $\tau_a \neq \tau_b$. The distribution of the site amplitudes in this case does not differ from the case with $m_P = m_Q$ and is governed by Eqs. (34) and (35). Although, the special choice of parameters here leads to the perfect resonance formation in the BIC regime.

Yet another feature, which is specific to the particular choice of the parameters, shown in Fig. 3 is a perfect transmission at the upper band edge, where the group velocity turns into zero. It results from the Van Hove singularity of DOS ($\rho \sim \frac{1}{\sqrt{2-\omega}}$)

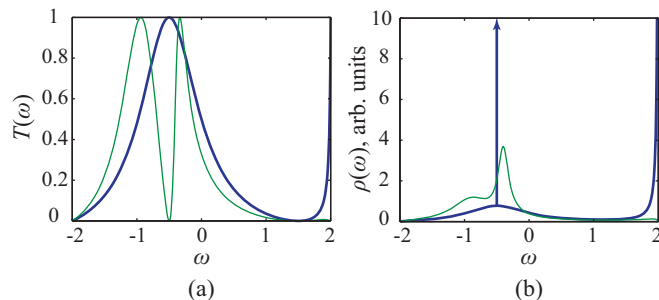


FIG. 3. BIC at perfect transmission energy. (a) Transmission coefficient of three-site system within the tight-binding approximation with $\tau_a = 1$ (thin green line) and $\tau_a = \frac{\sqrt{3}}{2\sqrt{2}}$ (thick blue line). (b) DOS for this structure [parameters are the same as in part (a)]. At $\tau_a = \frac{\sqrt{3}}{2\sqrt{2}}$, BIC appears and manifests itself as δ -function peak in the DOS. The perfect transmission and Van Hove singularity of DOS at the upper band edge are due to the real root of Q located exactly at this band edge. All values are in units of J .

and can be understood easily using the properties of P and Q functions. Indeed, with the parameters corresponding to BIC ($\tau_a = \tau_b$), one can see from Eq. (27) that the polynomial Q has a real root $\omega = 2\eta$. For our choice $\eta = 1$, we get that Q has a real root at the very upper band edge. Thus we have $Q \sim (2 - \omega)$ and $P \sim \sqrt{2 - \omega}$, and, consequently, at $\omega = 2$, perfect transmission takes place. The phenomenon of the perfect band edge transmission is common for real roots of Q falling at the very band edge with the Van Hove singularity.

C. BIC formation as “ghost phase transition” with abrupt symmetry transformation

In the preceding section for the particular three-site toy model, we obtained a singularity for the scattering state site amplitudes approaching the BIC point in the parameter space. Near BIC, the symmetry of the scattering state amplitudes at the sites forming BIC coincides with the symmetry of the BIC amplitudes. At the very BIC point, the symmetry of the scattering state amplitudes abruptly changes. Here we show that this singularity, which is the manifestation of an abrupt symmetry transformation, is a general property of the system in the parameter space region near BIC. We consider a point contact approximation and also assume leads to be semi-infinite linear chains with on-site energies set as the energy origin and nearest-neighbor hopping integral J set as the energy unit. The vector $\mathbf{a} = (a_1, \dots, a_N)^T$ of the site amplitudes can be found from the following equation:

$$\omega \hat{I} \mathbf{a} = \hat{H}_{\text{eff}} \mathbf{a} + \mathbf{s}, \quad (36)$$

where \hat{I} is the $N \times N$ identity matrix and \mathbf{s} is a “source vector.” Such form of the equation can be easily deduced from the results of Ref. [41]. In our case, the “source vector” is $\mathbf{s} = (s, 0, \dots, 0)^T$ with

$$s = \frac{2i}{\gamma_1^L} \Gamma_L. \quad (37)$$

From Eq. (36), we can straightforwardly find the site amplitudes:

$$\mathbf{a} = (\omega \hat{I} - \hat{H}_{\text{eff}})^{-1} \mathbf{s} = (\hat{A} + i\mathbf{u}_L \mathbf{u}_L^\dagger + i\mathbf{u}_R \mathbf{u}_R^\dagger)^{-1} \mathbf{s}. \quad (38)$$

Under the assumption of a point interaction, each of the vectors $\mathbf{u}_{L(R)}$ in the site localized states has only one nonzero element $u_{L,i} = \delta_{i1} \sqrt{\tilde{\Gamma}_L}$ and $u_{R,i} = \delta_{RN} \sqrt{\tilde{\Gamma}_R}$ correspondingly.

Next, we transform the basis to hybridized eigenstates of the structure, which diagonalize the matrix \hat{A} . For the sake of definiteness, we suppose that BIC originates from the state $|\tilde{1}\rangle$. It takes place as soon as the couplings $\tilde{u}_{L(R),\tilde{1}}$ vanish. Here tilde highlights the eigenstate basis. In the vicinity of this BIC, one can approximate the amplitude $\tilde{a}_{\tilde{1}}$ of the $|\tilde{1}\rangle$ state as

$$\tilde{a}_{\tilde{1}} \approx \frac{\alpha(\sqrt{\tilde{\Gamma}_L}, \sqrt{\tilde{\Gamma}_R})}{\Delta\omega + \beta(\sqrt{\tilde{\Gamma}_L}, \sqrt{\tilde{\Gamma}_R})}, \quad (39)$$

where $\Delta\omega = \omega - \tilde{\varepsilon}_{\tilde{1}}$, with $\tilde{\varepsilon}_{\tilde{1}}$ being the energy of the $|\tilde{1}\rangle$ state. In Eq. (39), $\alpha(x, y)$ is some linear form of x and y , $\beta(x, y)$ is some bilinear form of x and y , and $\tilde{\Gamma}_{L(R)} = |\tilde{u}_{L(R),\tilde{1}}|^2$. It should be noted here that the state $|\tilde{1}\rangle$ and, consequently, its energy $\tilde{\varepsilon}_{\tilde{1}} = \tilde{\varepsilon}_{\tilde{1}}(\tilde{u}_{L(R),\tilde{1}})$ naturally depend on the parameters of the system and, thus, this state turns into BIC just in the limit $\tilde{u}_{L(R),\tilde{1}} \rightarrow 0$ (or $\tilde{\Gamma}_{L(R)} \rightarrow 0$).

From Eq. (39), one can conclude that if one approaches the BIC energy by some trajectory in the energy-parameter space $\omega = \omega(\tilde{u}_{L(R),\tilde{1}})$ such that

$$\left. \frac{\partial\omega(\tilde{u}_{L(R),\tilde{1}})}{\partial\tilde{u}_{L(R),\tilde{1}}} \right|_{\tilde{u}_{L(R),\tilde{1}}=0} = \left. \frac{\partial\tilde{\varepsilon}_{\tilde{1}}(\tilde{u}_{L(R),\tilde{1}})}{\partial\tilde{u}_{L(R),\tilde{1}}} \right|_{\tilde{u}_{L(R),\tilde{1}}=0}, \quad (40)$$

then $\Delta\omega = \omega - \tilde{\varepsilon}_{\tilde{1}} = \mathcal{O}(|\tilde{u}_{L(R),\tilde{1}}|^2) = \mathcal{O}(\tilde{\Gamma}_{L(R)})$ and the amplitude of the scattering state $\tilde{a}_{\tilde{1}}$ formally diverges with the parameters tending to the BIC condition ($\tilde{u}_{L(R),\tilde{1}}, \tilde{\Gamma}_{L(R)} \rightarrow 0$). Figure 4(a) schematically illustrates this concept. This general description sheds light on the features of the behavior of the scattering state site amplitudes in the example considered in details in the previous subsection. It turned out that for BIC at $\eta = 0$ and $\omega = \varepsilon$ the trajectory, providing the formal divergence of the scattering state amplitudes is given by $\omega = \varepsilon'$ with ε' from Eq. (31), while for BIC at $\tau_a = \tau_b$ and $\omega = \varepsilon - \eta$ the diverging trajectory is simple (constant independent on $\tau_{a(b)}$): $\omega = \varepsilon - \eta$. Both this trajectories fulfill the condition (40), which is illustrated by Figs. 4(b) and 4(c), respectively. This approach generalizes previous results [76] about diverging the wave function in the vicinity of BIC in the interior of the system.

On the other hand, if the parameters satisfy the BIC condition ($\tilde{u}_{L(R),\tilde{1}} = 0$) exactly, the amplitude $\tilde{a}_{\tilde{1}}$ identically equals zero with a removable singularity at $\Delta\omega = 0$ ($\omega = \tilde{\varepsilon}_{\tilde{1}}$). Therefore, from the analysis of Eq. (39), we get that the distribution of the scattering state amplitudes in the vicinity of BIC corresponds to the distribution of the $|\tilde{1}\rangle$ state and it abruptly changes to the orthogonal one (such that $\tilde{a}_{\tilde{1}} = 0$), if the exact BIC condition is fulfilled. Thus BIC formation can be understood in some sense as a ‘‘phase transition’’ resulting in an abrupt symmetry transformation. In terms of the Landau theory of phase transitions, an incident wave can be considered as a field conjugated to the ‘‘order parameter’’ with the ‘‘order parameter’’ described by the BIC amplitude.

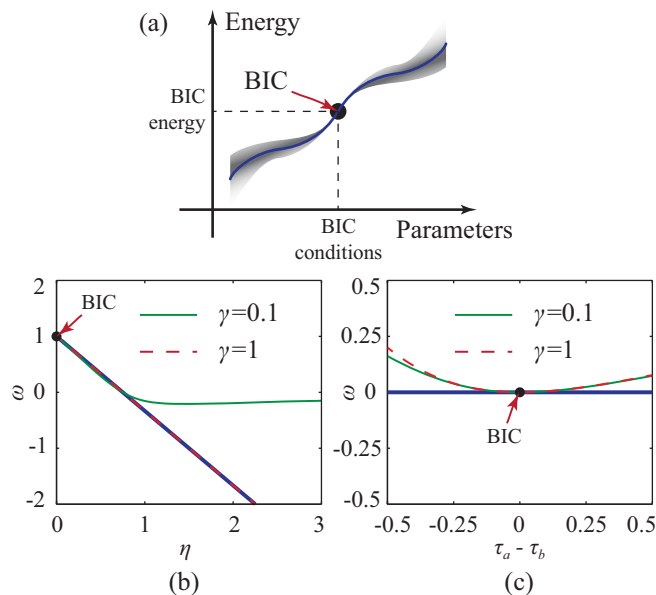


FIG. 4. Trajectories demonstrating scattering state amplitude divergence in energy-parameter space. (a) General view of trajectory of $\tilde{\varepsilon}_{\tilde{1}}(\tilde{u}_{L(R),\tilde{1}})$ (blue line) and schematic region (shaded), where trajectories $\omega(\tilde{u}_{L(R),\tilde{1}})$, providing formal divergence of scattering state amplitude, can pass. (b) Exact hybridized eigenenergies of three-site structure from the previous section in the vicinity of BIC at $\eta = 0$ and $\omega = \varepsilon$ with following parameters $\tau_a = 1$, $\tau_b = 0.5$, $\varepsilon = 1$, and $\gamma = 0.1$ (thin solid green line) or $\gamma = 1$ (thin dashed red line). Thick blue line corresponds to trajectory $\omega = \varepsilon'$. It is easily seen that this trajectory fulfills condition (40). (c) Exact hybridized eigenenergies of same structure in vicinity of BIC at $\tau_a = \tau_b$ and $\omega = \varepsilon - \eta$ with $\tau_b = 1$, $\varepsilon = 1$, $\eta = 1$, and $\gamma = 0.1$ (thin solid green line) or $\gamma = 1$ (thin dashed red line). Thick blue line corresponds to trajectory $\omega = \varepsilon - \eta$. In this case, the trajectory providing formal divergence is simple (constant) because the derivative of $\tilde{\varepsilon}_{\tilde{1}}$ in exact BIC is zero. All values are in units of J .

The diverging state amplitude $\tilde{a}_{\tilde{1}}$ here corresponds to the Curie-Weiss response function near the phase transition point.

V. ENGINEERING FANO RESONANCES: COALESCENCE OF RESONANCES AND ANTIRESONANCES

A. Quantum dot loop: generalized metacoupling with leads

In Refs. [29,42], the coalescence of perfect transmission maxima was shown to occur at the EP of the non-Hermitian auxiliary Hamiltonian. Here we focus on the coalescence of transmission zeros (antiresonances) and show that it can be related to an EP of some additional non-Hermitian Hamiltonian as well. We consider the structure, consisting of two equal N -site chains interconnected via the tunneling matrix element τ at the edge sites [Fig. 5(a)]. We numerate the sites in each chain from 1 to N , thus, the leads are connected to the first and to the N th site of the first chain via matrix elements γ_L and γ_R , correspondingly. Hence the number of the sites in these chains forming two branches of the loop differ by two and such coupling can be considered as a generalization of the metacoupling widely studied in aromatic molecules [79]. The Hamiltonian of the system we consider is

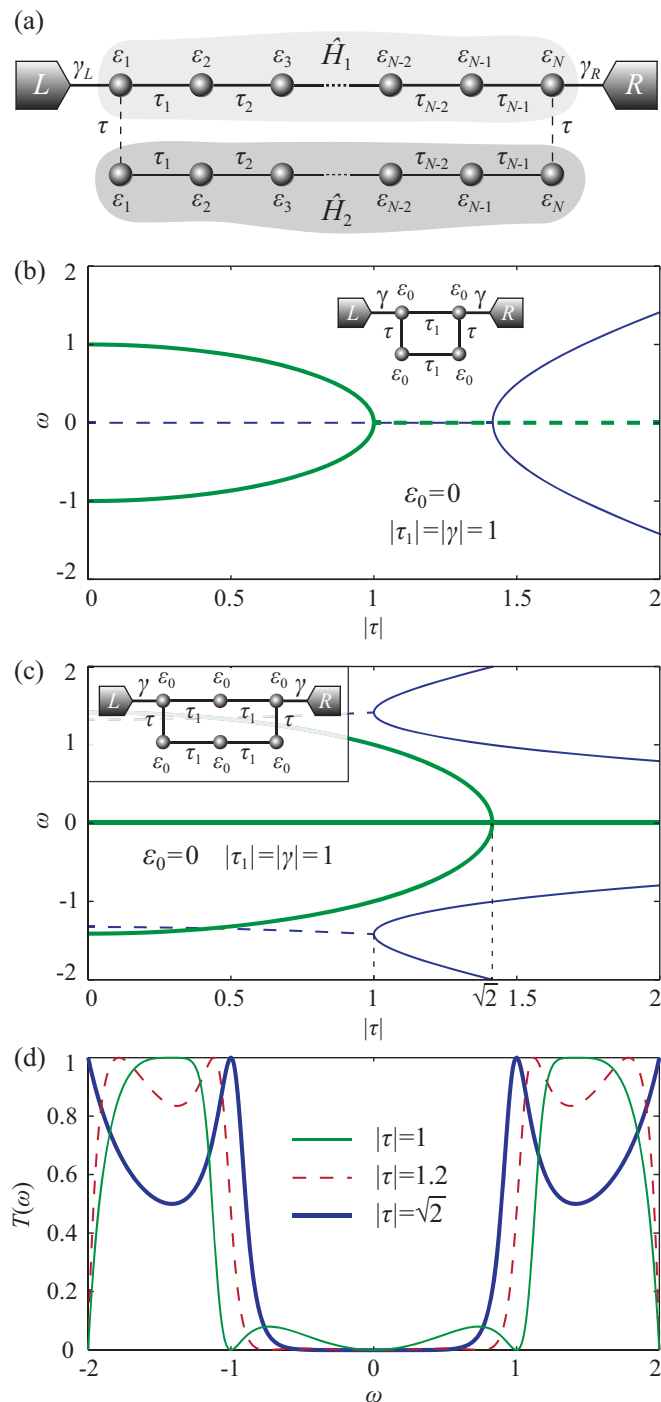


FIG. 5. Coalescence of antiresonances in double-chain structure. (a) Schematic view of double-chain structure. (b) and (c) Real parts of roots of $P(\omega)$ (thick green line) and real parts of roots of $Q(\omega)$ (thin blue line) calculated for $N = 2$ -site double-chain (b), which is shown in inset, and for $N = 3$ -site double-chain (c), which is also shown in inset. Solid lines show entirely real roots and dashed lines stand for real parts of complex roots. (d) Transmission coefficient profile in the very regime of antiresonance coalescence (thick blue line), in the very regime of resonance coalescence (thin green line) and in intermediate regime (thin dashed red line). All values are in units of J .

of general form (1) with a special choice of on-site energies ε_i and hopping integrals τ_{ij} . It is more convenient to write the bare Hamiltonian \hat{H}_0 of this structure in a block form:

$$\begin{aligned} \hat{H}_0 &= \hat{H}_1 + \hat{H}_2 + (\hat{\Omega}_{12} + \text{H.c.}), \\ \hat{H}_1 &= \sum_{i=1}^N \varepsilon_i a_i^\dagger a_i + \sum_{i=1}^{N-1} (\tau_i a_{i+1}^\dagger a_i + \text{H.c.}), \\ \hat{H}_2 &= \sum_{i=1}^N \varepsilon_i b_i^\dagger b_i + \sum_{i=1}^{N-1} (\tau_i b_{i+1}^\dagger b_i + \text{H.c.}), \\ \hat{\Omega}_{12} &= \tau b_1^\dagger a_1 + \tau b_N^\dagger a_N, \end{aligned} \quad (41)$$

where $a_i^\dagger(a_i)$ and $b_i^\dagger(b_i)$ are creation (annihilation) operators in the i th site of the first and the second chains, respectively. Here, $\hat{H}_{1(2)}$ corresponds to the Hamiltonian of the first (second) chain and $\hat{\Omega}_{12}$ describes the interaction between them.

Now we assume that the system is symmetric ($\tau_i = \tau_{N-i}$ and $\gamma_L = \gamma_R = \gamma$) and has identical on-site energies ($\varepsilon_i = \varepsilon_0$ for each i). Using Eq. (21), one can calculate the function P for this case (see Appendix B for details):

$$P = 2\sqrt{\Gamma_L \Gamma_R} \tau_1 \cdots \tau_{N-1} \det(\omega \hat{I} - \hat{H}_{\text{zero}}). \quad (42)$$

Here, \hat{H}_{zero} is a \mathcal{PT} -symmetric Hamiltonian defined in (B5); its real eigenvalues determine the transmission zeros just as the real eigenvalues of the auxiliary Hamiltonian (17) determine the perfect transmission energies. Thus, for the chains invariant under the mirror reflection and having identical on-site energies the coalescence of N zeros of transmission corresponding to the N th-order EP of the Hamiltonian \hat{H}_{zero} can take place. Hence, according to Ref. [29], the coalescence of an even number of transmission zeros results in a nonzero dip, whereas the coalescence of an odd number of zeros results in a zero-valued dip. According to the general relation (18), the transmission coefficient near the real N th-order root ω_0 of P takes the form

$$T(\omega) = \frac{(\omega - \omega_0)^{2N}}{(\omega - \omega_0)^{2N} + \tilde{\Gamma}^{2N}}, \quad (43)$$

where $\tilde{\Gamma}$ is, in general, an energy-dependent parameter and $\tilde{\Gamma}(\omega_0) \neq 0$.

As an illustration, we consider two N -site double-chain structures with $N = 2$ and $N = 3$. Leads in both cases are treated as semi-infinite linear chains with the hoping integral J set as the energy unit. Figure 5(b) shows the real roots and real parts of the complex roots of P and Q for the two-site double chain as functions of $|\tau|$. We set $|\tau_1| = |\gamma| = 1$ and $\varepsilon_0 = 0$. Figure 5(c) corresponds to the three-site double chain. Here we again assume $|\tau_1| = |\gamma| = 1$ and $\varepsilon_0 = 0$. Coalescence of the real roots of P [shown by thick green lines in Figs. 5(b) and 5(c)] indeed corresponds to the coalescence of transmission zeros, because it takes place at the nonzero point of Q . For the particular examples considered, it is not difficult to derive conditions for the coalescence of antiresonances: $|\tau| = 1$ for the two-site double-chain structure [Fig. 5(b)] and $|\tau| = \sqrt{2}$ for the three-site double-chain structure [Fig. 5(c)]. These plots also demonstrate the difference between the coalescence of even and odd number of antiresonances mentioned above.

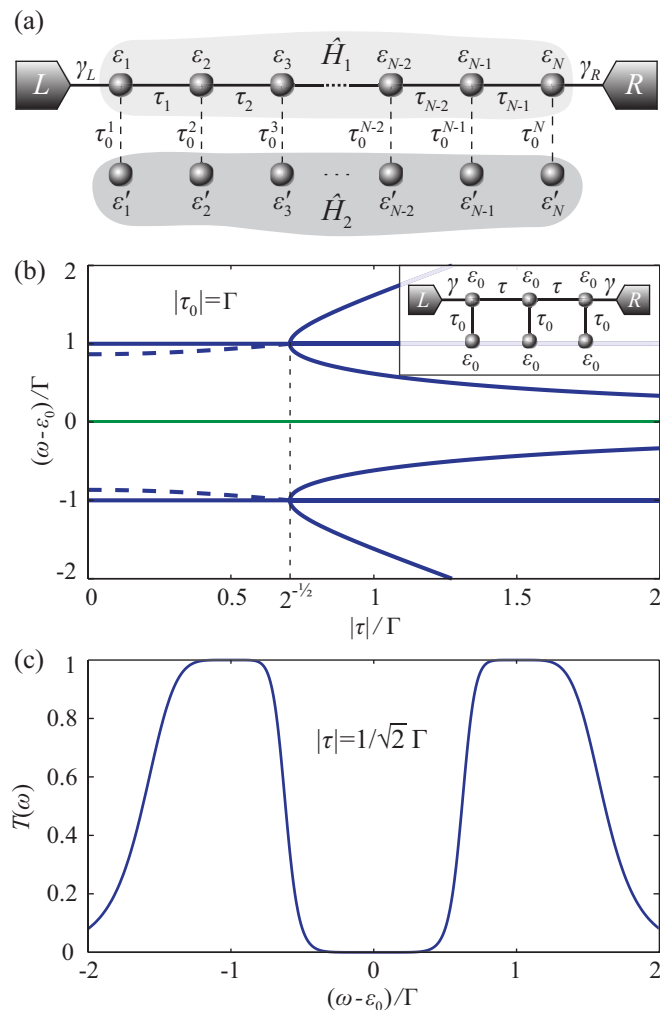


FIG. 6. Coalescence of Fano resonances and antiresonances in a comblike structure. (a) Schematic view of the comblike structure. (b) Positions of real parts of roots of $P(\omega)$ (thin green line) and real parts of roots of $Q(\omega)$ (thick blue line) calculated for $N = 3$ -site comblike structure (shown in inset) in the wide-band limit. Solid lines show entirely real roots and dashed lines stand for real parts of complex roots. Parameter $|\tau_0|$ is set to 1. One can see that coalescence of resonances takes place at $|\tau| = \frac{1}{\sqrt{2}}\Gamma$. (c) Transmission coefficient profile in the very regime of the resonance coalescence.

$$P = 2\tilde{\omega}^N \Gamma \tau_1 \cdots \tau_{N-1}, \quad Q = \begin{vmatrix} (\tilde{\omega} - \delta - i\Gamma)\tilde{\omega} - |\tau_0|^2 & -\tau_1\tilde{\omega} & \cdots & 0 & 0 \\ -\tau_1^*\tilde{\omega} & \tilde{\omega}^2 - |\tau_0|^2 & \cdots & 0 & 0 \\ \vdots & \vdots & \ddots & \vdots & \vdots \\ 0 & \cdots & \tilde{\omega}^2 - |\tau_0|^2 & -\tau_{N-1}\tilde{\omega} & 0 \\ 0 & \cdots & -\tau_{N-1}^*\tilde{\omega} & (\tilde{\omega} - \delta + i\Gamma)\tilde{\omega} - |\tau_0|^2 & 0 \end{vmatrix}, \quad (45)$$

where $\tilde{\omega} = \omega - \varepsilon_0$.

From Eq. (45), it is clear that $\omega = \varepsilon_0$ ($\tilde{\omega} = 0$) is the N th-order root of P and $Q(\tilde{\omega} = 0) \neq 0$, hence $\omega = \varepsilon_0$ is the N th-order zero of transmission. This is a crossing point of Fano resonance minima. In the wide-band limit (or Fermi golden rule approximation) [26], there can also be a coalescence of Fano resonance maxima in this structure. Under this

Figure 5(d) shows transmission versus energy profiles for the three-site double-chain structure. These profiles are plotted for three values of $|\tau|$ representing the coalescence of antiresonances ($|\tau| = \sqrt{2}$), coalescence of two pairs of resonances ($|\tau| = 1$), and in some intermediate position ($|\tau| = 1.2$). For $|\tau| = \sqrt{2}$, there are perfect transmission points at the band edges, which are due to the real roots of Q , located exactly at the band edges [see Fig. 5(c)].

B. Quantum dot comblike structure: Crossing of antiresonances

Consider a comblike structure representing an N -site linear chain with side-defect sites connected to each site of the chain [Fig. 6(a)]. It is also more convenient to write the bare Hamiltonian of this structure in a block form:

$$\begin{aligned} \hat{H}_0 &= \hat{H}_1 + \hat{H}_2 + (\hat{\Omega}_{12} + \text{H.c.}), \\ \hat{H}_1 &= \sum_{i=1}^N \varepsilon_i a_i^\dagger a_i + \sum_{i=1}^{N-1} (\tau_i a_{i+1}^\dagger a_i + \text{H.c.}), \\ \hat{H}_2 &= \sum_{i=1}^N \varepsilon'_i b_i^\dagger b_i, \\ \hat{\Omega}_{12} &= \sum_{i=1}^N \tau_0^i b_i^\dagger a_i. \end{aligned} \quad (44)$$

Here, a_i^\dagger (a_i) is the creation (annihilation) operator in the i th site of the chain with the energy ε_i and b_i^\dagger (b_i) is the creation (annihilation) operator in the i th side-defect site with the energy ε'_i connected to the i th site of the chain via the hopping integral τ_0^i .

We assume that all sites of the linear chain and all side-defect sites are physically identical, i.e., have the same energy: $\varepsilon'_i = \varepsilon_i = \varepsilon_0$, also we suppose that $\tau_0^1 = \cdots = \tau_0^N = \tau_0$. The leads are treated as identical and are connected to the 1-st and to the N th site of the chain by the matrix elements $\gamma_L = \gamma_R = \gamma$ (resulting in $\Gamma_L = \Gamma_R = \Gamma$ and $\delta_L = \delta_R = \delta$). In this case, the functions P and Q can be derived in the following form (see Appendix C for details):

assumption, $\delta \approx 0$ and $\Gamma \approx \gamma^2/J \approx \text{const}$ is independent of energy. Here, J is a half of the bandwidth in the leads, which we treat to be much greater than the difference between the energies of our interest (ω, ε_0) and the center of the leads' band. According to Eq. (45), coalescence of transmission peaks can take place at the energy $\omega = \varepsilon_0 \pm |\tau_0|$ for a certain ratio between the tunneling matrix elements τ_i

[29,42]. Thus one can tune the parameters of the structure in such a way that its transmission coefficient will have the N th-order zero dip surrounded by two N th-order unity peaks. Figure 6(b) shows the positions of the real parts of the roots of the functions Q and P for the three-site comblike structure calculated in the wide-band limit. Coalescence of three real roots of Q forms an EP of the third order, which corresponds to the coalescence of resonances. Figure 6(c) depicts the corresponding profile of the transmission coefficient energy dependence in the very regime of the coalescence of resonances.

VI. SUMMARY

In this paper, we have presented a general description of resonances, antiresonances, and BICs via the unique formalism. Our observation is that a dissipationless but open quantum system possesses features such as EP and \mathcal{PT} -symmetry breaking, which are common to systems with balanced gain and loss terms in the corresponding non-Hermitian effective Hamiltonian. In the theory of OQS, the eigenstates of the non-Hermitian effective Hamiltonian are the resonant states, which describe unstable quantum states [1,18,19]. Here we showed that non-Hermitian Hamiltonians can be very useful also in the description of the stationary scattering resonances in OQS. We have found out that for an arbitrary two-terminal multiply connected molecular (or QD) conductor or waveguide, the square module of the characteristic determinant of the effective Hamiltonian (denominator in the expression for the transparency) can be written in a simple form of a sum of two non-negative terms. The first term is a square module of the characteristic determinant of the auxiliary Hamiltonian; its zeros (i.e., eigenvalues of the auxiliary Hamiltonian) determine the transparency peaks. The second term is an energy- (frequency-) dependent function that is exactly the numerator in the expression for the transparency and its zeros determine antiresonances. The non-Hermitian auxiliary Hamiltonian can be easily deduced from the Feshbach effective non-Hermitian Hamiltonian and differs from it by the implementation of the scattering boundary conditions instead of the Siegert ones. We should emphasize that this approach is useful only for scattering problems, whereas in describing resonant states and decay problems the traditional effective Hamiltonian based description is preferable. The presented theory is formulated for one-dimensional systems, or more accurately—for 1-manifolds, i.e., systems with only one continuous variable (wave vector k in the leads) and a finite number of discrete variables (number of branches). Nevertheless, this theory is applicable to three-dimensional systems, which allows for variable separation and can be described by a one-dimensional model. Examples of such systems are planar semiconductor heterostructures [23,27,29], photonic crystals [3,80], etc.

The resonances and BICs are related to the complex and real eigenvalues of the effective Hamiltonian, correspondingly. However, a complex eigenvalue of the effective Hamiltonian, which is a pole of the scattering matrix, in general, does not determine the position of the resonance on the energy axis exactly. The real eigenvalues of the auxiliary Hamiltonian that coincide with the real eigenvalues of the effective

Hamiltonian determine BICs. The real eigenvalues of the auxiliary Hamiltonian that do coincide with the real eigenvalues of the effective Hamiltonian determine the exact positions of perfect resonances on the energy axis. The EPs of the auxiliary Hamiltonian are responsible for the coalescence of resonances. It should be noted also that in this paper all calculations were carried out within a localized orthogonal basis (constructed, for example, by Löwdin orthogonalization [81]). On the other hand, in numerical simulations of real quantum molecular conductors (e.g., in DFT), the basis of the Hamiltonian eigenstates, which diagonalizes the initial Hamiltonian of the isolated structure, is more convenient. It can be shown that in the diagonal basis antiresonances are described by the nondiagonal non-Hermitian coupling in the effective Hamiltonian [15,69,73,82,83].

Scattering states and BICs are deeply coupled to each other. As we have shown, the symmetry (mutual interrelation) of the scattering state amplitudes on the sites corresponding to BIC exactly coincides with the symmetry of the BIC amplitudes near the BIC point in the parameter space. A trajectory in the generalized energy-parameter space can be chosen such that on this trajectory the absolute value of the scattering state amplitude diverges while approaching the BIC point. At the very BIC point, the structure of the scattering state amplitudes changes abruptly and the scattering state wave function (waveguide mode) becomes orthogonal to BIC. This picture closely resembles the behavior of the system near the point of the second-order phase transition with BIC being the order parameter, the scattering state wave function being the conjugated field and the scattering state amplitudes at the BIC sites—the generalized response function obeying the Curie-Weiss-like law. Our model does not account for the interelectron Coulomb interactions, which can be partially justified under the assumption of strong coupling with the leads resulting in small values of the site amplitudes inside the molecule. However, for electromagnetic fields in waveguides, the description is adequate for large site amplitudes as well. Hence our model provides a straightforward approach for creating a BIC and a storage of intense fields by an abrupt switching from the scattering regime to BIC and vice versa. It should be noted also that recently in Ref. [84], it has been shown that BICs do survive with interelectron interactions being taken into account at least in Coulomb blockade regime.

The obtained results, which relate resonance and BIC energies to the problem of finding real roots of well-defined energy functions, make it possible to control the positions of perfect and zero transmission as well as their coalescence. Thus our results could be helpful for the deduction of the design rules for quantum conductors and waveguides. For example, one can convert the perfect transmission into the zero transmission (or vice versa) at the same energy by tuning some structures' parameters. As an example of the application of such design rules we have constructed two families of quantum structures: an asymmetric loop with symmetric branches (generalized metacoupling to the leads) and a symmetric comb-like structure. Both families exhibit coalescence of antiresonances resulting in formation of a broad reflection window. In the former structure, an almost rectangle window of transparency, described in Ref. [29],

is converted into an almost rectangle window of reflectivity (43) just by adding the same single-channel wire in parallel. Such rectangle windows of transmission can be applied [85] within the area of quantum heat engines [86,87]. Other fields of possible applications are the design of broad-band filters [88] and photonic crystals [89,90] formed by 2D periodic arrays of dielectric rods with an in-plane light wave, which is polarized along these rods [80]. In particular, one can get the transmission dips or peaks by adding or removing defects close to the main waveguide. Moreover, one can create

both a transmission window or a reflection window using single-chain and double-chain structures, correspondingly. Thus, with the same lithographic template, both structures can be realized.

ACKNOWLEDGMENTS

A.A.G. would like to acknowledge the Program of Fundamental Research of the Presidium of the Russian Academy of Sciences No. 1 for partial support.

APPENDIX A: DENSITY OF STATES NEAR BIC

Here we show that for an arbitrary QD system described by the Hamiltonian (1) formation of BIC results in appearance of a δ -function peak of the density of states (DOS). DOS can be derived straightforwardly from the retarded Green function of the system (6):

$$\rho(\omega) = -\frac{1}{\pi} \text{Im} \sum_i G_{ii}^r = -\frac{1}{\pi} \text{Im} \text{Tr} \hat{G}^r, \quad (\text{A1})$$

where summation runs through all sites of the structure. In terms of the matrix \hat{A} and vectors $\mathbf{u}_{L(R)}$, introduced in Sec. III, DOS can be written as

$$\rho(\omega) = -\frac{1}{\pi} \text{Im} \text{Tr} (\hat{A} + i\mathbf{u}_L \mathbf{u}_L^\dagger + i\mathbf{u}_R \mathbf{u}_R^\dagger)^{-1}. \quad (\text{A2})$$

Using the Sherman-Morrison formula [66] and matrix determinant lemma [67], one can get the explicit expression for DOS in the following form:

$$\rho(\omega) = \frac{1}{\pi} \frac{R(\omega)}{|P(\omega)|^2 + |Q(\omega)|^2} \quad (\text{A3})$$

with P and Q defined by Eqs. (14) and (16) and

$$R = (\det \hat{A})^2 \{ \mathbf{u}_L^\dagger \hat{A}^{-2} \mathbf{u}_L [1 + (\mathbf{u}_R^\dagger \hat{A}^{-1} \mathbf{u}_R)^2] + \mathbf{u}_R^\dagger \hat{A}^{-2} \mathbf{u}_R [1 + (\mathbf{u}_L^\dagger \hat{A}^{-1} \mathbf{u}_L)^2] - 2(\mathbf{u}_L^\dagger \hat{A}^{-1} \mathbf{u}_L + \mathbf{u}_R^\dagger \hat{A}^{-1} \mathbf{u}_R) \text{Re} [\mathbf{u}_R^\dagger \hat{A}^{-1} \mathbf{u}_L \mathbf{u}_L^\dagger \hat{A}^{-2} \mathbf{u}_R] + |\mathbf{u}_R^\dagger \hat{A}^{-1} \mathbf{u}_L|^2 (\mathbf{u}_L^\dagger \hat{A}^{-2} \mathbf{u}_L + \mathbf{u}_R^\dagger \hat{A}^{-2} \mathbf{u}_R) \}. \quad (\text{A4})$$

BIC is a localized state, which is totally decoupled from the continuum of states in the leads. Thus, in the basis of the eigenstates of the structure hybridized by the leads (i.e., in the basis, which diagonalizes the matrix \hat{A}), BIC can be understood as a state $|\tilde{n}\rangle$, such that its coupling to the leads $\tilde{\gamma}_{\tilde{n}}^{L(R)}$ vanishes as well as the corresponding (n th) element of the vector $\tilde{\mathbf{u}}_{L(R)}$ [15]. Here tilde highlights the diagonalized basis.

Now consider DOS in the vicinity of BIC. Suppose that $\tilde{\varepsilon}_{\tilde{1}}, \dots, \tilde{\varepsilon}_{\tilde{N}}$ are the eigenenergies of the hybridized structure, and we assume for definiteness that BIC appears at the energy $\omega = \tilde{\varepsilon}_{\tilde{1}}$, when the parameters $\tilde{u}_{L(R),\tilde{1}}$ tend to zero. In this case, the matrix \hat{A} is diagonal with $A_{\tilde{i}\tilde{i}} = (\omega - \tilde{\varepsilon}_{\tilde{i}})$. In the vicinity of BIC, we can assume $\Delta\omega = \omega - \tilde{\varepsilon}_{\tilde{1}}$ and $\tilde{\Gamma}_{L(R)} = |\tilde{u}_{L(R),\tilde{1}}|^2$ to be small compared to $\min_{\tilde{i},\tilde{j}} |\tilde{\varepsilon}_{\tilde{i}} - \tilde{\varepsilon}_{\tilde{j}}|$ and $\min_{\tilde{i}} |\tilde{u}_{L(R),\tilde{i}}|^2$, correspondingly. Treating $\tilde{\Gamma}_{L(R)}$ and $\Delta\omega$ as small quantities of the same order, one can approximate $\rho(\omega)$ in the vicinity of BIC as

$$\rho(\omega) \approx \frac{1}{\pi} \frac{\beta_1(\sqrt{\tilde{\Gamma}_L}, \sqrt{\tilde{\Gamma}_R})}{[\Delta\omega + \beta_2(\sqrt{\tilde{\Gamma}_L}, \sqrt{\tilde{\Gamma}_R})]^2 + [\beta_3(\sqrt{\tilde{\Gamma}_L}, \sqrt{\tilde{\Gamma}_R})]^2}, \quad (\text{A5})$$

where $\beta_i(a,b)$ are some bilinear forms of a and b . From Eq. (A5), it is clear that in the limit $\tilde{\Gamma}_{L(R)} \rightarrow 0$ DOS in the vicinity of BIC has a δ -function peak.

APPENDIX B: DERIVATION OF FUNCTION P FOR DOUBLE-CHAIN STRUCTURE

To calculate the function P for a double-chain structure, we use Eq. (21), where the minor M_{1N} of $(\omega\hat{I} - \hat{H}_{\text{eff}})$ is needed. According to Eq. (41), the Hamiltonian of the isolated system \hat{H}_0 and, consequently, the effective Hamiltonian \hat{H}_{eff} can be presented as a 2×2 block matrix:

$$\hat{H}_{\text{eff}} = \begin{pmatrix} \hat{H}_1^{\text{eff}} & \hat{\Omega}_{12} \\ \hat{\Omega}_{12}^\dagger & \hat{H}_2 \end{pmatrix}. \quad (\text{B1})$$

Here, \hat{H}_1^{eff} is the Hamiltonian of the first chain with the leads self-energies taken into account. Applying the rules of block matrix inversion [91] (or equivalently the Löwdin partitioning technique [81]) one can calculate the necessary minor and get the

following expression for the function P :

$$P = 2\sqrt{\Gamma_L \Gamma_R} \det(\omega \hat{I} - \hat{H}_2) \cdot \begin{vmatrix} -\tau_1 & 0 & 0 & \dots & 0 & 0 & -|\tau|^2 [(\omega \hat{I} - \hat{H}_2)^{-1}]_{1N} \\ \omega & -\tau_2 & 0 & \dots & 0 & 0 & 0 \\ -\tau_2^* & \omega & -\tau_3 & \dots & 0 & 0 & 0 \\ \vdots & \vdots & \vdots & \ddots & \vdots & \vdots & \vdots \\ 0 & 0 & 0 & \dots & -\tau_{N-3} & 0 & 0 \\ 0 & 0 & 0 & \dots & \omega & -\tau_{N-2} & 0 \\ 0 & 0 & 0 & \dots & -\tau_{N-2}^* & \omega & -\tau_{N-1} \end{vmatrix}. \quad (\text{B2})$$

The matrix element $[(\omega \hat{I} - \hat{H}_2)^{-1}]_{1N}$ is derived from Eq. (41):

$$[(\omega \hat{I} - \hat{H}_2)^{-1}]_{1N} = \frac{\tau_1 \cdots \tau_{N-1}}{\det(\omega \hat{I} - \hat{H}_2)}. \quad (\text{B3})$$

Substituting (B3) into (B2) and expanding the determinant by the first row one can simplify P in the following way:

$$\begin{aligned} P &= 2\sqrt{\Gamma_L \Gamma_R} \det(\omega \hat{I} - \hat{H}_2) \left[(-1)^{N-1} \tau_1 \cdots \tau_{N-1} - (-1)^N |\tau|^2 \frac{\tau_1 \cdots \tau_{N-1}}{\det(\omega \hat{I} - \hat{H}_2)} D_1^1 \right] \\ &= 2\sqrt{\Gamma_L \Gamma_R} \cdot (-1)^{N-1} \tau_1 \cdots \tau_{N-1} [\det(\omega \hat{I} - \hat{H}_2) + |\tau|^2 D_1^1]. \end{aligned} \quad (\text{B4})$$

Here, D_q^p stands for the minor of the $(\omega \hat{I} - \hat{H}_1)$ matrix with the first p rows and columns and the last q rows and columns crossed out. As chains are equal, we can also think of D_q^p as the corresponding minor of the $(\omega \hat{I} - \hat{H}_2)$ matrix.

Now we use the fact that the double-chain structure under study is symmetric. In this case, we can conclude that the expression in the square brackets in Eq. (B4) is the determinant of the matrix $(\omega \hat{I} - \hat{H}_{\text{zero}})$, where \hat{H}_{zero} is the following \mathcal{PT} -symmetric Hamiltonian:

$$(\hat{H}_{\text{zero}})_{mn} = (\hat{H}_2)_{mn} + i|\tau|(\delta_{m1}\delta_{n1} - \delta_{mN}\delta_{nN}). \quad (\text{B5})$$

Indeed, this can be checked directly by expanding the determinant of $(\omega \hat{I} - \hat{H}_{\text{zero}})$:

$$\det(\omega \hat{I} - \hat{H}_{\text{zero}}) = \det(\omega \hat{I} - \hat{H}_2) + i|\tau|(D_0^1 - D_1^0) + |\tau|^2 D_1^1. \quad (\text{B6})$$

In a symmetric structure, minors D_0^1 and D_1^0 are equal and from Eq. (B6) we get exactly the expression in the square brackets in the right-hand side of Eq. (B4).

As was mentioned in the Sec. III, P is defined up to an arbitrary phase factor. Thus we can neglect the sign in Eq. (B4) and get the polynomial P for the symmetric double-chain model in the form (42).

APPENDIX C: DERIVATION OF FUNCTIONS P AND Q FOR COMB-LIKE STRUCTURE

As it was done for the double-chain structure, in the case of a comblike structure, we can again write the effective Hamiltonian in the block form (B1), but with \hat{H}_1 , \hat{H}_2 , and $\hat{\Omega}_{12}$ taken from Eq. (44). Such form of the effective Hamiltonian allows us to calculate P easily:

$$P = 2\sqrt{\Gamma_L \Gamma_R} \tau_1 \cdots \tau_{N-1} (\omega - \varepsilon'_1) \cdots (\omega - \varepsilon'_N). \quad (\text{C1})$$

Function Q can be derived in a similar way, because the auxiliary Hamiltonian also has a block matrix form. Thus, according to Eq. (21) and, once again, using the block matrix inversion rules from Ref. [91], one can get that

$$Q = \begin{vmatrix} \omega - \varepsilon_1 - \delta_L - i\Gamma_L - \frac{|\tau_0^1|^2}{\omega - \varepsilon'_1} & -\tau_1 & \dots & 0 & 0 \\ -\tau_1^* & \omega - \varepsilon_2 - \frac{|\tau_0^2|^2}{\omega - \varepsilon'_2} & \dots & 0 & 0 \\ \vdots & \vdots & \ddots & \vdots & \vdots \\ 0 & 0 & \dots & \omega - \varepsilon_{N-1} - \frac{|\tau_0^{N-1}|^2}{\omega - \varepsilon'_{N-1}} & -\tau_{N-1} \\ 0 & 0 & \dots & -\tau_{N-1}^* & \omega - \varepsilon_N - \delta_R + i\Gamma_R - \frac{|\tau_0^N|^2}{\omega - \varepsilon'_N} \end{vmatrix} \\ \times (\omega - \varepsilon'_1) \cdots (\omega - \varepsilon'_N). \quad (\text{C2})$$

Assuming that $\varepsilon'_i = \varepsilon_i = \varepsilon_0$, $\tau_0^1 = \cdots = \tau_0^N = \tau_0$ and the leads are identical, we simplify Eqs. (C1) and (C2) to Eq. (45).

- [1] N. Moiseyev, *Non-Hermitian Quantum Mechanics* (Cambridge University Press, Cambridge, 2011).
- [2] F. Monticone and A. Alù, *Rep. Prog. Phys.* **80**, 036401 (2017).
- [3] A. E. Miroshnichenko, S. Flach, and Y. S. Kivshar, *Rev. Mod. Phys.* **82**, 2257 (2010).
- [4] C. W. Hsu, B. Zhen, A. D. Stone, J. D. Joannopoulos, and M. Soljačić, *Nat. Rev. Mater.* **1**, 16048 (2016).
- [5] L. D. Landau and E. M. Lifshitz, *Quantum Mechanics: Non-Relativistic Theory* (Elsevier, Oxford, 2013), Vol. 3.
- [6] H. Feshbach, *Ann. Phys.* **5**, 357 (1958); **19**, 287 (1962); **43**, 410 (1967).
- [7] J. Von Neuman and E. Wigner, *Phys. Z.* **30**, 467 (1929).
- [8] H. Friedrich and D. Wintgen, *Phys. Rev. A* **32**, 3231 (1985).
- [9] A. Kodigala, T. Lepetit, Q. Gu, B. Bahari, Y. Fainman, and B. Kanté, *Nature (London)* **541**, 196 (2017).
- [10] I. Rotter and A. F. Sadreev, *Phys. Rev. E* **71**, 046204 (2005).
- [11] Y. Plotnik, O. Peleg, F. Dreisow, M. Heinrich, S. Nolte, A. Szameit, and M. Segev, *Phys. Rev. Lett.* **107**, 183901 (2011).
- [12] A. F. Sadreev, E. N. Bulgakov, and I. Rotter, *J. Phys. A: Math. Gen.* **38**, 10647 (2005).
- [13] G. Ordóñez, K. Na, and S. Kim, *Phys. Rev. A* **73**, 022113 (2006).
- [14] E. N. Bulgakov and A. F. Sadreev, *Phys. Rev. B* **81**, 115128 (2010).
- [15] M. L. Ladrón de Guevara and P. A. Orellana, *Phys. Rev. B* **73**, 205303 (2006).
- [16] J.-X. Yan and H.-H. Fu, *Physica B: Condens. Matter* **410**, 197 (2013).
- [17] J. Okołowicz, M. Płoszajczak, and I. Rotter, *Phys. Rep.* **374**, 271 (2003).
- [18] I. Rotter, *J. Phys. A: Math. Theor.* **42**, 153001 (2009).
- [19] I. Rotter and J. P. Bird, *Rep. Prog. Phys.* **78**, 114001 (2015).
- [20] N. Hatano, K. Sasada, H. Nakamura, and T. Petrosky, *Prog. Theor. Phys.* **119**, 187 (2008).
- [21] M. Müller and I. Rotter, *Phys. Rev. A* **80**, 042705 (2009).
- [22] H. Eleuch and I. Rotter, *Phys. Rev. A* **95**, 022117 (2017).
- [23] A. Gorbatshevich, M. Zhuravlev, and V. Kapaev, *J. Exp. Theor. Phys.* **107**, 288 (2008).
- [24] W. Vanroose, *Phys. Rev. A* **64**, 062708 (2001).
- [25] T. Belozerova and V. Henner, *Phys. Part. Nuclei* **29**, 63 (1998).
- [26] A. D. Dente, R. A. Bustos-Marín, and H. M. Pastawski, *Phys. Rev. A* **78**, 062116 (2008).
- [27] R. Romo and G. García-Calderón, *Phys. Rev. B* **49**, 14016 (1994).
- [28] M. Müller, F.-M. Dittes, W. Iskra, and I. Rotter, *Phys. Rev. E* **52**, 5961 (1995).
- [29] A. Gorbatshevich and N. Shubin, *Ann. Phys.* **376**, 353 (2017).
- [30] G. Khitrova, H. M. Gibbs, M. Kira, S. W. Koch, and A. Scherer, *Nat. Phys.* **2**, 81 (2006).
- [31] T. Stehmann, W. D. Heiss, and F. G. Scholtz, *J. Phys. A: Math. Gen.* **37**, 7813 (2004).
- [32] J. Schindler, A. Li, M. C. Zheng, F. M. Ellis, and T. Kottos, *Phys. Rev. A* **84**, 040101 (2011).
- [33] D. Cardamone, C. Stafford, and B. Barrett, *Phys. Status Solidi (b)* **230**, 419 (2002).
- [34] E. Danielli, G. Álvarez, P. Levstein, and H. Pastawski, *Solid State Commun.* **141**, 422 (2007).
- [35] C. M. Bender and S. Boettcher, *Phys. Rev. Lett.* **80**, 5243 (1998); C. M. Bender, S. Boettcher, and P. N. Meisinger, *J. Math. Phys.* **40**, 2201 (1999); C. M. Bender, *Rep. Prog. Phys.* **70**, 947 (2007).
- [36] A. Guo, G. J. Salamo, D. Duchesne, R. Morandotti, M. Volatier-Ravat, V. Aimez, G. A. Siviloglou, and D. N. Christodoulides, *Phys. Rev. Lett.* **103**, 093902 (2009).
- [37] C. E. Ruter, K. G. Makris, R. El-Ganainy, D. N. Christodoulides, M. Segev, and D. Kip, *Nat. Phys.* **6**, 192 (2010).
- [38] F. Cannata, J.-P. Dedonder, and A. Ventura, *Ann. Phys.* **322**, 397 (2007).
- [39] H. Hernandez-Coronado, D. Krejčířk, and P. Siegl, *Phys. Lett. A* **375**, 2149 (2011).
- [40] L. Jin and Z. Song, *Phys. Rev. A* **81**, 032109 (2010).
- [41] L. Jin and Z. Song, *J. Phys. A: Math. Theor.* **44**, 375304 (2011).
- [42] A. A. Gorbatshevich and N. M. Shubin, *JETP Lett.* **103**, 769 (2016).
- [43] T. Kato, *Perturbation Theory for Linear Operators*, Classics in Mathematics (Springer-Verlag, Berlin, Heidelberg, 1995).
- [44] W. D. Heiss, *J. Phys. A: Math. Gen.* **37**, 2455 (2004); *J. Phys. A: Math. Theor.* **45**, 444016 (2012).
- [45] M. Berry, *Czech. J. Phys.* **54**, 1039 (2004).
- [46] J. Wiersig, *Phys. Rev. A* **93**, 033809 (2016).
- [47] A. Mostafazadeh, *J. Math. Phys.* **43**, 205 (2002).
- [48] S. V. Suchkov, F. Fotsa-Ngaffo, A. Kenfack-Jiotsa, A. D. Tikeng, T. C. Kofane, Y. S. Kivshar, and A. A. Sukhorukov, *New J. Phys.* **18**, 065005 (2016).
- [49] A. Regensburger, C. Bersch, M.-A. Miri, G. Onishchukov, D. N. Christodoulides, and U. Peschel, *Nature (London)* **488**, 167 (2012).
- [50] H. Alaïan and J. A. Dionne, *Phys. Rev. A* **89**, 033829 (2014).
- [51] A. Mostafazadeh, *Ann. Phys.* **368**, 56 (2016).
- [52] M. Liertzer, L. Ge, A. Cerjan, A. D. Stone, H. E. Türeci, and S. Rotter, *Phys. Rev. Lett.* **108**, 173901 (2012); M. Brandstetter, M. Liertzer, C. Deutsch, P. Klang, J. Schöberl, H. E. Türeci, G. Strasser, K. Unterrainer, and S. Rotter, *Nat. Commun.* **5**, 4034 (2014).
- [53] S. Longhi, *Phys. Rev. A* **82**, 031801 (2010).
- [54] W. D. Heiss and G. Wunner, *Eur. Phys. J. D* **68**, 284 (2014).
- [55] W. Vanroose, P. V. Leuven, F. Arickx, and J. Broeckhove, *J. Phys. A: Math. Gen.* **30**, 5543 (1997).
- [56] P. Ambichl, K. G. Makris, L. Ge, Y. Chong, A. D. Stone, and S. Rotter, *Phys. Rev. X* **3**, 041030 (2013).
- [57] Y. D. Chong, L. Ge, and A. D. Stone, *Phys. Rev. Lett.* **106**, 093902 (2011).
- [58] E. N. Bulgakov, K. N. Pichugin, A. F. Sadreev, and I. Rotter, *JETP Lett.* **84**, 430 (2006).
- [59] C. Blanchard, J.-P. Hugonin, and C. Sauvan, *Phys. Rev. B* **94**, 155303 (2016).
- [60] K. Okamoto, *Fundamentals of Optical Waveguides* (Academic Press, Burlington, San Diego, 2010).
- [61] S. Longhi, *Laser Photon. Rev.* **3**, 243 (2009).
- [62] C. Caroli, R. Combescot, P. Nozieres, and D. Saint-James, *J. Phys. C* **4**, 916 (1971).
- [63] S. Datta, *Electronic Transport in Mesoscopic Systems*, Cambridge Studies in Semiconductor Physics (Cambridge University Press, Cambridge, 1997).
- [64] D. Ryndyk, R. Gutiérrez, B. Song, and G. Cuniberti, in *Energy Transfer Dynamics in Biomaterial Systems* (Springer-Verlag, Berlin, Heidelberg, 2009), pp. 213–335.
- [65] V. V. Sokolov and V. G. Zelevinsky, *Ann. Phys.* **216**, 323 (1992).
- [66] J. Sherman and W. J. Morrison, *Ann. Math. Stat.* **21**, 124 (1950).

- [67] D. A. Harville, *Matrix Algebra from a Statistician's Perspective* (Springer, New York, NY, 1997), Vol. 1.
- [68] U. Fano, *Phys. Rev.* **124**, 1866 (1961).
- [69] S. Tanaka, S. Garmon, K. Kanki, and T. Petrosky, *Phys. Rev. A* **94**, 022105 (2016).
- [70] H. Lu, R. Lü, and B.-f. Zhu, *Phys. Rev. B* **71**, 235320 (2005).
- [71] W. Gong, Y. Han, and G. Wei, *J. Phys.: Condens. Matter* **21**, 175801 (2009).
- [72] K. Sasada, N. Hatano, and G. Ordonez, *J. Phys. Soc. Jpn.* **80**, 104707 (2011).
- [73] M. L. Ladrón de Guevara, F. Claro, and P. A. Orellana, *Phys. Rev. B* **67**, 195335 (2003).
- [74] P. A. Orellana, M. L. Ladrón de Guevara, and F. Claro, *Phys. Rev. B* **70**, 233315 (2004).
- [75] C. S. Kim, A. M. Satanin, Y. S. Joe, and R. M. Cosby, *Phys. Rev. B* **60**, 10962 (1999).
- [76] A. F. Sadreev, E. N. Bulgakov, and I. Rotter, *Phys. Rev. B* **73**, 235342 (2006).
- [77] E. Bulgakov and A. Sadreev, *Phys. Rev. B* **83**, 235321 (2011).
- [78] See Supplemental Material at <http://link.aps.org/supplemental/10.1103/PhysRevB.96.205441> for the application of the theory to several models of BIC formed in a Fabry-Perot resonator.
- [79] M. Smith, *Organic Chemistry: An Acid-Base Approach* (Taylor and Francis, Boca Raton, 2011).
- [80] S. F. Mingaleev and Y. S. Kivshar, *Opt. Lett.* **27**, 231 (2002); S. F. Mingaleev, Y. S. Kivshar, and R. A. Sammut, *Phys. Rev. E* **62**, 5777 (2000); S. Flach, A. E. Miroshnichenko, V. Fleurov, and M. V. Fistul, *Phys. Rev. Lett.* **90**, 084101 (2003); A. E. Miroshnichenko and Y. S. Kivshar, *Phys. Rev. E* **72**, 056611 (2005).
- [81] P.-O. Löwdin, *J. Chem. Phys.* **18**, 365 (1950); *J. Math. Phys.* **3**, 969 (1962); *J. Mol. Spectrosc.* **10**, 12 (1963).
- [82] H. Vaupel, P. Thomas, O. Kühn, V. May, K. Maschke, A. P. Heberle, W. W. Rühle, and K. Köhler, *Phys. Rev. B* **53**, 16531 (1996).
- [83] S. Longhi, *J. Mod. Opt.* **56**, 729 (2009).
- [84] M. A. Sierra, M. Saiz-Bretín, F. Domínguez-Adame, and D. Sánchez, *Phys. Rev. B* **93**, 235452 (2016).
- [85] C. H. Schiegg, M. Dzierzawa, and U. Eckern, *J. Phys.: Condens. Matter* **29**, 085303 (2017).
- [86] R. Kosloff and A. Levy, *Annu. Rev. Phys. Chem.* **65**, 365 (2014).
- [87] R. S. Whitney, *Phys. Rev. B* **91**, 115425 (2015).
- [88] W. Menzel, L. Zhu, K. Wu, and F. Bogelsack, *IEEE Trans. Microwave Theory Tech.* **51**, 364 (2003); X. Zhou, X. Yin, T. Zhang, L. Chen, and X. Li, *Opt. Express* **23**, 11657 (2015).
- [89] J. D. Joannopoulos, P. R. Villeneuve, and S. Fan, *Nature (London)* **386**, 143 (1997).
- [90] Y. Yu, Y. Chen, H. Hu, W. Xue, K. Yvind, and J. Mork, *Laser Photon. Rev.* **9**, 241 (2015).
- [91] B. Noble and J. Daniel, *Applied Linear Algebra* (Prentice Hall Inc., Englewood Cliffs, NJ, 1977).